Pergamon

Int. J. Heat Mass Transfer. Vol. 40, No. 17, pp. 4043–4053, 1997

Printed in Great Britain
0017–9310/97 $17.00+0.00

PII: S0017–9310(97)00051–3

Experimental route to heat conduction beyond the Fourier equation

P. GUILLEMET, J. P. BARDON and C. RAUCH

Laboratoire de Thermocinétique de l'ISITEM, Rue Christian Pauc, La Chantrerie, CP 90604, 44306 NANTES Cedex 03, France

(*Received* 3 *October* 1996 *and in final form* 14 *February* 1997)

Abstract—The theory and implementation of an experiment aimed at studying heat behavior on a very short time scale (up to 10^{-11} s) is explained. A detailed thermal model, based on the hyperbolic heat conduction equation, shows that a non-diffusive (or even oscillating) heat behavior with relaxation time influence (in Vernotte's meaning) needs to be considered. There is also some discussion about the theoretical problem of compatibility with the second law of thermodynamics. The first results from the validation stage, concerning the 'slow' version of the experiment (time scale: 10^{-9}–10^{-6} s), are presented. Work on the 'fast' version is currently in progress. © 1997 Elsevier Science Ltd.

1. RESEARCH FRAMEWORK

New thermal problems are appearing with the recent developments in the fields of micro- and nano-technologies and with the use of ultra-short pulse laser. They are related to high power density leading to strong heat dissipation in these systems. A clear understanding of the dissipation phenomena and unsteady heat transfer within microsystems and nanostructures, in the nano- pico- or femto-second time scale, is quite an important research subject.

In these extreme conditions, the Fourier law is no longer valid, and a new approach in modelling and experimentation is necessary. Recently, many theoretical studies, gathering specialists of thermal science, solid physics, optics and thermodynamics, have suggested new heat propagation equations. As of yet, no experimentation has accepted the challenge of experimental validation of these equations or experimental determination of the 'relaxation times' defined therein.

We are proposing and implementing an experimental device with the aim of studying the very first instants of heat propagation, up to 10^{-11} s. We assume that the notion of temperature exists up to 10^{-12} s and can be used to investigate the heat behavior on the same order of time as most materials relaxation time. An estimation of relaxation times from Ref. [1] is summarized in Fig. 1.

2. PRINCIPLE OF EXPERIMENTATION

2.1. *Choice criterion*

The main problems that arise when entering the 'non-Fourier' domain are:

(1) The time scale is very short and out of the bandwidth of most electronic devices.
(2) The space scale must be very small (under 1 μm) to obtain high temperature gradients. The spatial resolution required is not attainable with classical thermal sensors.
(3) The finite temperature speed variation, due to finite heating power in a very short time, only produces a weak available energy. Thus, high sensitivity sensors are needed. Unfortunately, they are often the slowest, for the same reason: the ratio of detected energy/detection duration remains finite even when the detection duration is very short.

It was desired to design the most optimal and least restrictive device. It is feasible to utilize the device for further experimentation with other materials and for other time or space scales. The three problems mentioned above have led to three necessary procedures:

(1) The breaking down of signal recording, similar to stroboscopic lighting of the temperature field, with a delay line technique (in the 'fast' version of the experiment, detailed in Section 4.1).
(2) The extension of the spatial zone available for analysis, by spatial periodical repetition of the phenomena (two laser beams interference).
(3) The time periodical repetition of the experiment using a pulsed laser for the heating stage.

2.2. *Our choice: the forced Rayleigh scattering (F.R.S.)*

An old method has been chosen and fitted to our purpose: the forced Rayleigh scattering (F.R.S.), based on a light scattering by a transient phase grating. Formerly used to measure thermal diffusivity [2], it is still active in transient phenomena research [3, 4]. This method has been adapted to thick-sample

NOMENCLATURE

e	sample thickness [m]
k	thermal conductivity [W m^{-1} K^{-1}]
l	interfringe [m]
n	medium refractive index
T	temperature [K]
t	time [s]
y	space abscissa [m].

Dimensionless variables

T^*	$=T/\Delta T_0$
t^*	$=\alpha \cdot t/l^2$
τ^*	$=\alpha \cdot \tau/l^2$
y^*	$=y/l$.

Greek symbols

α	thermal diffusivity [m^2 s^{-1}]
ΔT	sinusoidal temperature field amplitude [K]
ΔT_0	initial temperature field amplitude, right after the end of heating stage [K]
ϕ	heat flux [W/m^2]
φ	angle between the two heating beams [rad]
λ_{pump}	heating beam wavelength [m]
λ_{probe}	probe beam wavelength [m]
η	diffraction efficiency
τ	relaxation time [s].

experimentation in order to be able to study weak absorption media, such as natural diamond or sapphire, chosen because of their very high thermal diffusivity that leads to ultra-fast thermal transient phenomenon.

A semi-transparent sample is first instantaneously heated with two coherent laser pulses, interfering in the volume. The interference pattern is a spatial sinusoidal intensity modulation: it creates alternating dark and bright zones that produce, by light absorption, cold and hot zones. The distance between two hot zones is the interfringe:

$$l = \frac{\lambda_{pump}}{2\sin\left(\frac{\varphi}{2}\right)}.$$

In our experiment, l can vary from 0.3 to 30 μm.

Following the heating stage, heat propagation causes a decreasing temperature field amplitude ΔT, and finally cancels it (see Fig. 2).

Because the refractive index is a function of temperature, it is spatially modulated in the medium. Thus, the sample behaves like a phase grating towards a third beam (probe beam) being propagated through the temperature field. A luminous signal is then obtained in the diffraction pattern during the whole experiment duration.

For a thick sample and a weak temperature amplitude ΔT, the diffraction efficiency is given by:

$$\eta = \frac{\text{Diffracted beam intensity}}{\text{Probe beam intensity}} = \left(\frac{\pi \frac{dn}{dT}\Delta T \cdot e}{\lambda_{probe} n}\right)^2.$$

The probe beam intensity and other parameters of this formula (e, dn/dT, λ_{probe}, n) are constant: they do not need to be measured. A continuous and high speed real time measurement of the diffracted beam intensity gives the time dependence of DT:

$$\Delta T(t) = K\sqrt{\text{Diffracted beam intensity}(t)} \quad (1)$$

with K being an unknown constant. An arbitrary unit temperature field amplitude (ΔT) is then obtained. The only intensity to be measured is the diffracted

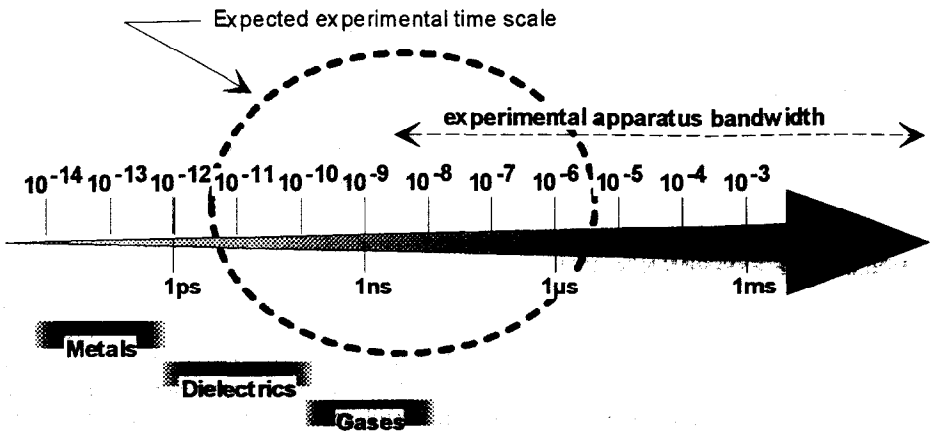

Fig. 1. Relaxation time estimation (dotted line: our experimental time scale).

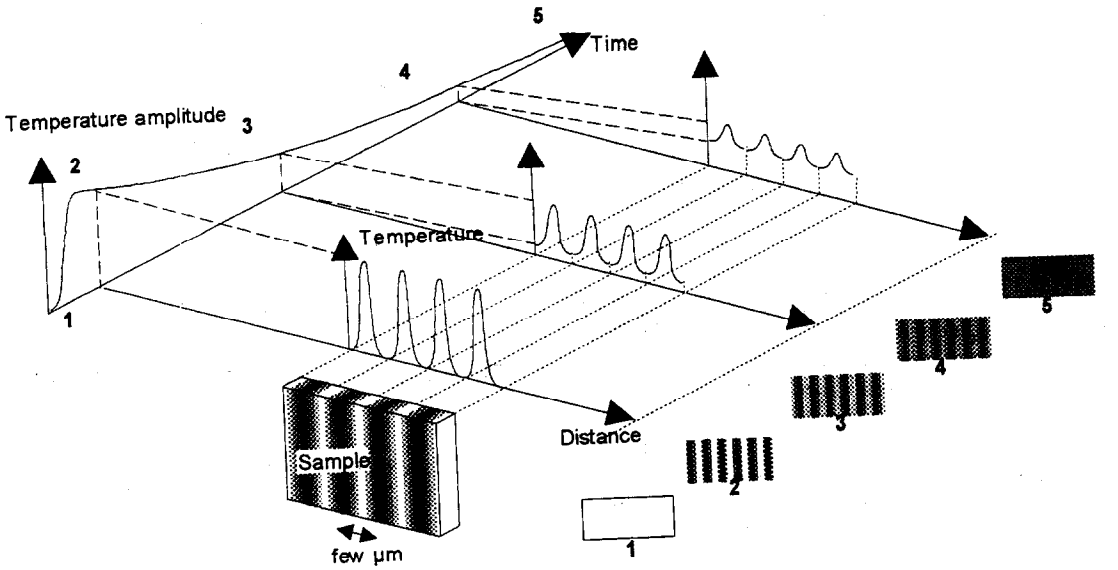

Fig. 2. Principle of the experimentation.

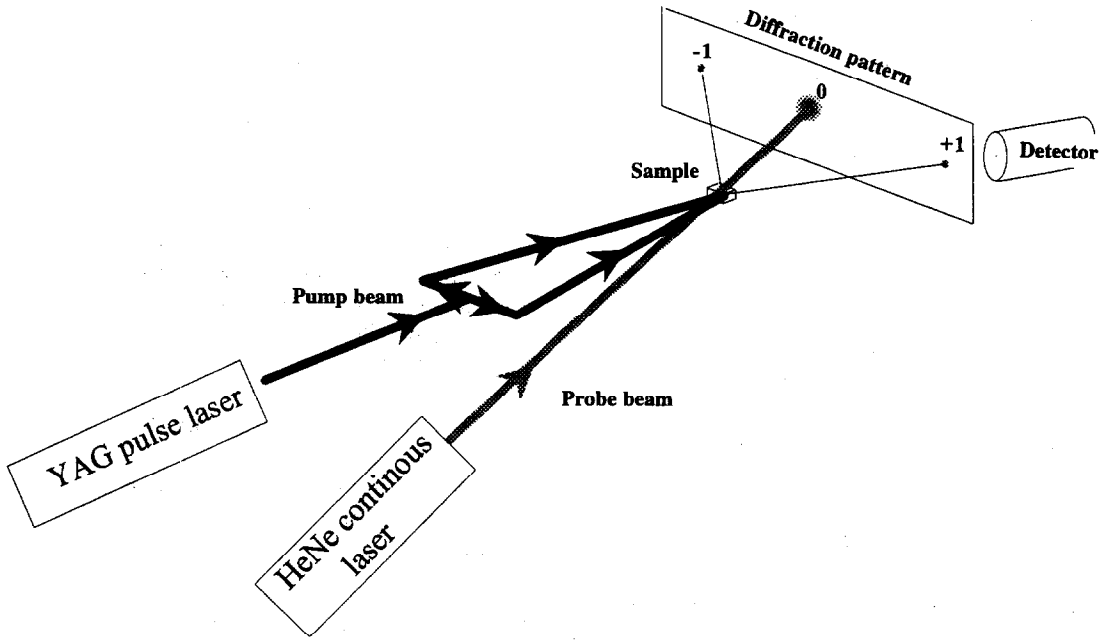

Fig. 3. Pump and probe beams ('slow' version).

beam intensity. The measurement takes place in the first order of the diffraction pattern (see Fig. 3).

3. THERMAL MODEL: BEYOND THE FOURIER EQUATION

It has been known and emphasized for half a century that the Fourier equation predicts an instantaneous propagation of heat in the sense that a whole medium should be (following this equation) instantaneously affected by a local perturbation of the temperature field. This is physically unacceptable. To remove this paradox, a relaxation time, or delay time, between heat flux and temperature gradient was proposed by Carlo Cattaneo and Pierre Vernotte in 1958 [5–7]:

$$\phi(t) = -k\nabla T + \tau\frac{\delta\phi}{\delta t}.$$

The modified Fourier equation combined with the energy balance equation, leads to a hyperbolic heat equation.

$$\tau\frac{\partial^2 T(y,t)}{\partial t^2} + \frac{\partial T(y,t)}{\partial t} - \alpha\frac{\partial^2 T(y,t)}{\partial y^2} = 0. \quad (2)$$

This hyperbolic model has been the subject of numer-

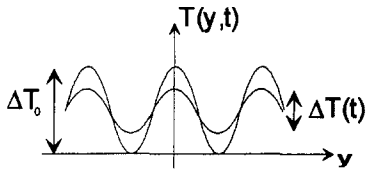

Fig. 4. Notations and temperature field diagram.

ous studies and papers (Ref. [8] gives an overview of them). Though other models are available, the hyperbolic heat equation has been used in our computations, as there are many theories which validate it.

Since between two fringes heat transfer occurs mainly in the direction normal to the fringe, we assume a one-dimensional phenomenon in the y-direction. Four boundary conditions are needed: two in space, two in time. The initial temperature field is imposed by the two pump interfering pulses absorption. The spatial shape of this field is the one of the interference field, which is sinusoidal with a period equal to l, the interfringe (see Fig. 4):

$$T(y,0) = \frac{\Delta T_0}{2}\left(\sin\left(\frac{2\pi y}{l}\right)+1\right).$$

The other boundary conditions are:

$$\frac{\partial T(y,0)}{\partial t} = 0$$

$$\frac{\partial T(0,t)}{\partial y} = 0$$

$$\frac{\partial T(l,t)}{\partial y} = 0.$$

Because of the initial distribution, it is more easy to use:

$$T' = T - \frac{\Delta T_0}{2}.$$

Using dimensionless variables, $T^* = T'/\Delta T_0$, $y^* = y/l$, $t^* = \alpha \cdot t/l^2$ and $\tau^* = \alpha \cdot \tau/l^2$ the system can be written as:

$$\tau^*\frac{\partial^2 T^*}{\partial t^{*2}} + \frac{\partial T^*}{\partial t^*} - \frac{\partial^2 T^*}{\partial y^{*2}} = 0$$

$$T^*(y^*,0) = \tfrac{1}{2}\sin(2\pi y^*)$$

$$\frac{\partial T^*(y^*,0)}{\partial t^*} = 0$$

$$\frac{\partial T^*(0,t^*)}{\partial y^*} = 0$$

$$\frac{\partial T^*(1,t^*)}{\partial y^*} = 0. \qquad (3)$$

Solutions can be found using a classical decomposition:

$$T^*(y^*,t^*) = \Delta T(t^*)\cdot g(y^*).$$

Equation (3) becomes:

$$\tau^*\frac{1}{\Delta T^*}\frac{\mathrm{d}^2\Delta T^*}{\mathrm{d}t^{*2}} + \frac{1}{\Delta T^*}\frac{\mathrm{d}\Delta T^*}{\mathrm{d}t^*} = \frac{1}{g}\frac{\mathrm{d}^2 g}{\mathrm{d}y^{*2}}.$$

The space dependence of T^* is:

$$g(y^*) = \tfrac{1}{2}\cos(2\pi y^*).$$

The time dependence of T^* is the solution of equation (4):

$$\tau^*\frac{\mathrm{d}^2\Delta T^*}{\mathrm{d}t^{*2}} + \frac{\mathrm{d}\Delta T^*}{\mathrm{d}t^*} + 4\pi^2\Delta T^* = 0. \qquad (4)$$

The solution is:

$$\Delta T^*(t^*) = Ae^{m_1 t^*} + Be^{m_2 t^*}$$

with m_1 and m_2 solutions of:

$$\tau^* r^2 + r + 4\pi^2 = 0.$$

Depending on whether the discriminant D of this last equation is positive (case 1 and 2) or negative (case 3), real or imaginary solutions are obtained, leading to an exponentially decreasing or a deadened oscillatory amplitude:

Case 1: $\tau^* \approx 0$

$$\Delta T^*(t^*) = \exp(-4\pi^2 t^*). \qquad (5)$$

This solution is, of course, the solution of the parabolic heat equation.

Case 2: $\tau^* < 1/16\pi^2$

$$\Delta T^*(t^*) = \frac{1+\sqrt{D}}{2\sqrt{D}}\exp\left(\frac{-1+\sqrt{D}}{2\tau^*}t^*\right) + \frac{-1+\sqrt{D}}{2\sqrt{D}}\exp\left(\frac{-1-\sqrt{D}}{2\tau^*}t^*\right). \qquad (6)$$

Case 3: $\tau^* > 1/16\pi^2$

$$\Delta T^*(t^*) = \frac{1}{\cos(\varphi)}\exp\left(\frac{-t^*}{2\tau^*}\right)\cos\left(\frac{\sqrt{-D}}{2\tau^*}t^* + \varphi\right)$$

$$\text{with:}\quad \tan(\varphi) = \frac{-1}{\sqrt{-D}}. \qquad (7)$$

Case 1 (or 2) and 3 lead to quite different heat behavior.

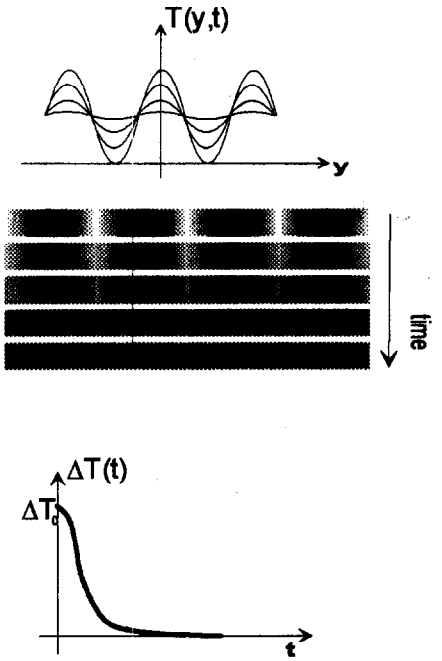

Fig. 5. Classical diffusion (hot zones in dark).

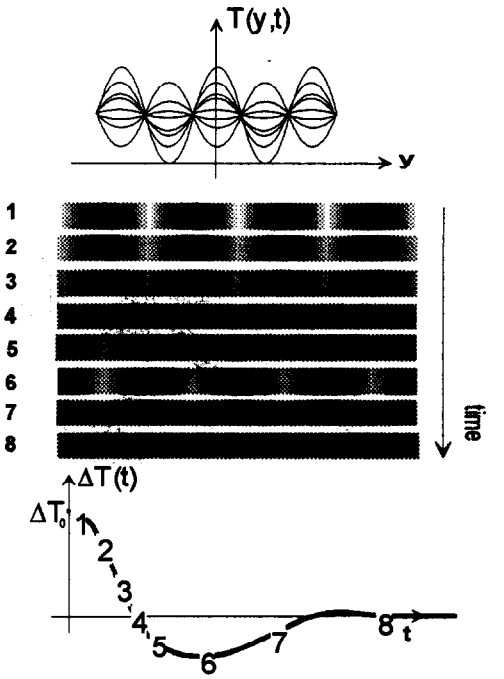

Fig. 6. Wave propagation with deadening.

Case 1 or 2, as shown in the computation of Fig. 5, gives a classical behavior. It is perfectly diffusive when $\tau = 0$ or lightly hyperbolic when τ is weak. It is a non-periodic solution.

Case 3, as shown in Fig. 6, gives an amazing deadening oscillatory behavior when the product $\tau \times \alpha$ is great enough. This quasi-periodical solution is induced by the insertion of a relaxation time in the heat equation. The term $\tau^* \partial^2 T^*/\partial t^{*2}$ of the hyperbolic heat equation is a typical deadening term of an oscillating system. In the hyperbolic equation, this behavior is observed when inertia (τ) is great enough (say not negligible compared to the experiment time scale) and when deadening ($1/\alpha$) is weak enough.

The relaxation oscillations predicted by case 3 seem to contradict the second law of thermodynamics. In situation 5 (Fig. 6) a strange heat flux appears from a cold to a hot zone, which should not be physically possible. In situation 4, the temperature gradient is null but the heat flux is not.

This type of contradiction, related to the 'memory' or 'inertial' effect of the relaxation time, has already been underlined by many authors (Refs. [1, 9] for example) and is actually an important subject of theoretical research. To remove the contradiction, a new definition of temperature, heat flux and entropy is suggested by the new developments of extended irreversible [10]. Our purpose is not theoretical, we are attempting to perform the experiments in the greatest range of the product $\tau^* \alpha$ as possible, in order to watch heat behavior and to try to compare it to any available model. Moreover, the device has been designed to show a possible 'non-Fourier' effect even in the non-periodical solution of case 2. For example, computation of Fig. 7, at time 2×10^{-8} s, with a 2.5×10^{-5} m^2 s^{-1} diffusivity sample, a 6 μm interfringe and a 9×10^{-9} s relaxation time, leads to a 14% difference between the parabolic and hyperbolic model. It is

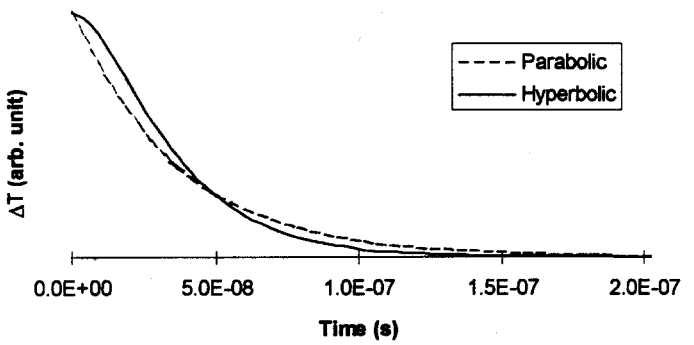

Fig. 7. Non-Fourier effect in non-periodical propagation.

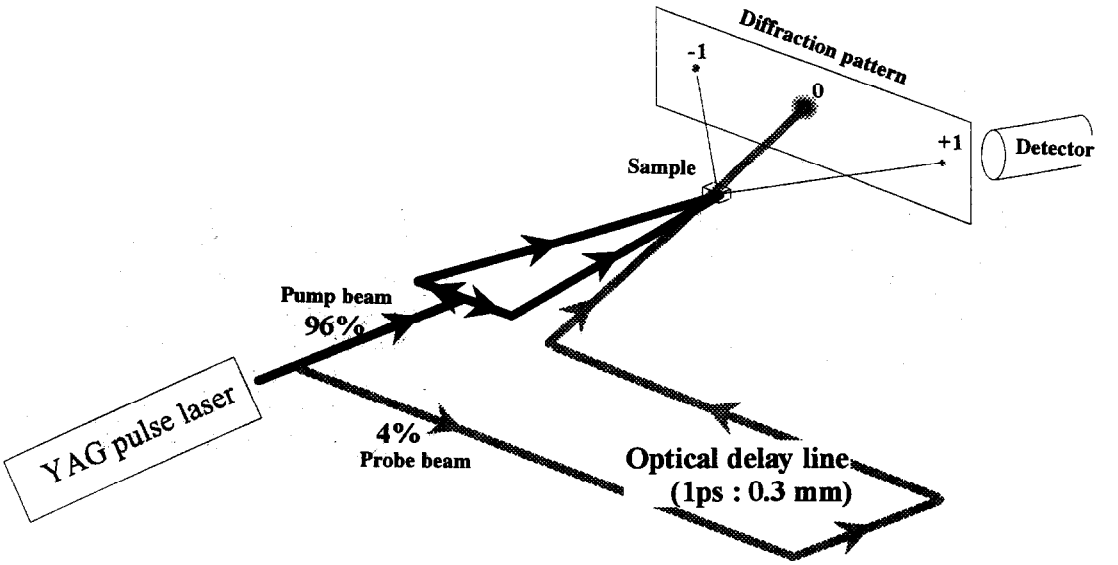

Fig. 8. Pump and probe beams ('fast' version).

quite possible to validate this calculation with the present experimental apparatus.

4. EXPERIMENTATION APPARATUS

4.1. *The two versions of the experiment*

The experimentation, of which the principle is presented in Section 2.2, is the 'slow' version of the experiment. The diffracted intensity varies very quickly. Its measurement is possible only up to the upper limit of best detector bandwidth. Because of the comparatively small value of detector rise time (say about 1 ns for a high-sensitivity photomultiplier), it is not possible to reach the expected 10 ps of Fig. 1 with this 'slow' experiment version.

To lower the time resolution, a breaking down of the recorded signal is used in the other version of the experiment called the 'fast' version. The probe beam is itself a laser pulse, synchronized with the pump pulse (see Fig. 8). At the moment the probe beam goes through the sample, the diffraction gives a single value of ΔT, a sort of snapshot of the temperature field. This snap can be recorded with an integrating detector, which is slow but very much less sensitive to fast transient electromagnetic perturbations. This pump and probe technique is often used in fast transient phenomenon and is well described in Ref. [4].

In fact, the probe beam is a part of the pump beam, optically taken with a beam splitter. The numerous points needed to restore the entire curve (ΔT vs time) are obtained from numerous experiments. Each experiment gives an average result for one point in time. From one experiment to another, the probe pulse is more and more delayed by means of an optical delay line, giving results for increasing times.

4.2. *Technical description*

When not focused, the pump and beam diameter is 1 mm FWHM. This is the diameter of the cylindrical tested sample zone (see Fig. 9) which includes about one thousand interfringes and where the average temperature field amplitude is measured.

Table 1 gives the main typical features of both the slow and fast versions of the experimental procedure. The YAG laser can produce either a 17 ns pulse with a Pockels cell or a 35 ps pulse with a saturable absorber. The wavelength can be either 1064 or 532 nm using a KTP single harmonic generator. The whole optical device, including the sample, is locked up in a black and airtight cage to avoid lighting of detectors by any ray except those from the diffraction pattern. The low level electrical output of detector and ampli-

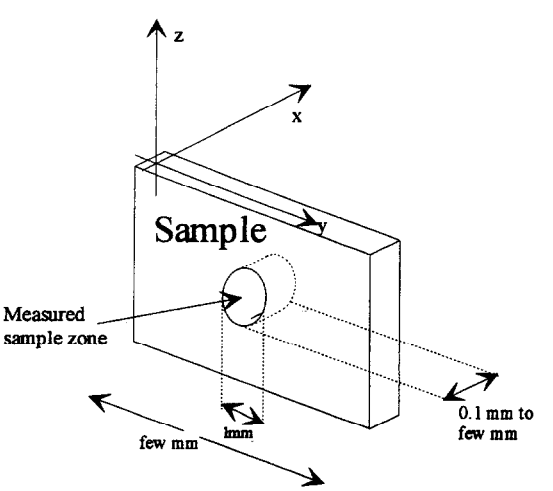

Fig. 9. Dimensions of sample.

Table 1. Technical data

	'Slow' version	'Fast' version
Pump		
Pulse duration	17 ns	35 ps
Energy per pulse	400 mJ	1 mJ
Repetition rate	10 Hz	10 Hz
Probe		
Laser	He–Ne (633 nm)	YAG (1064 nm)
Power	5 mW	4% of pump pulse
Detection		
Detector	Silicon photodiode or photomultiplier (R6427 Hamamatsu)	Pyroelectric or silicon joulemeter (J25 or J3S10 Molectron)
Rise time	1.5 ns	Integrating detector
Amplifier	0–400 MHz, 40 dB	None
Digital scope	Random sampling, 500 Ms s^{-1}; 5000 data, 2 bytes (Tektronics TDS 420 A)	

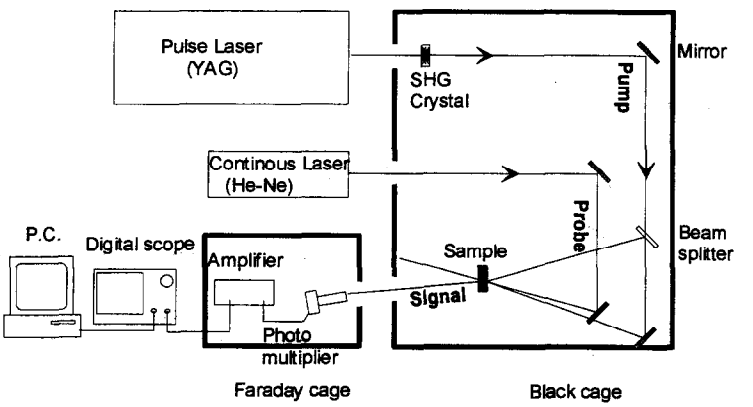

Fig. 10. 'Slow' version experimental schematic.

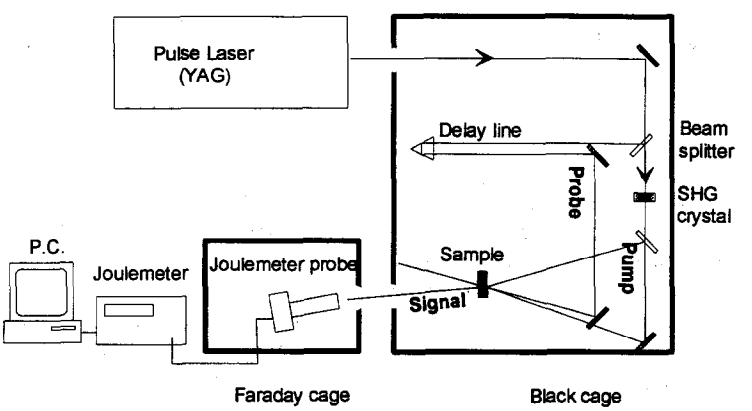

Fig. 11. 'Fast' version experimental schematic.

fier is protected from interference by a high efficiency Faraday cage (see Figs. 10 and 11).

5. EXPERIMENTATION ADVANCEMENT

5.1. *Some difficulties*

Technical difficulties are not lacking, of course. Figure 12 shows the huge difference between the pump and diffracted beam power, which have to be separated by the detector. The diffracted beam weakness is a consequence of the small absorption value of the used material causing a weak ΔT, and of the very low dn/dT coefficient (typically 10^{-7} K^{-1}) which is the origin of the phase grating. The refractive index variation is about 0.00001%. Under these conditions, it is imperative to reach the minimum limit of noise. That is very difficult because of the unavoidable strong

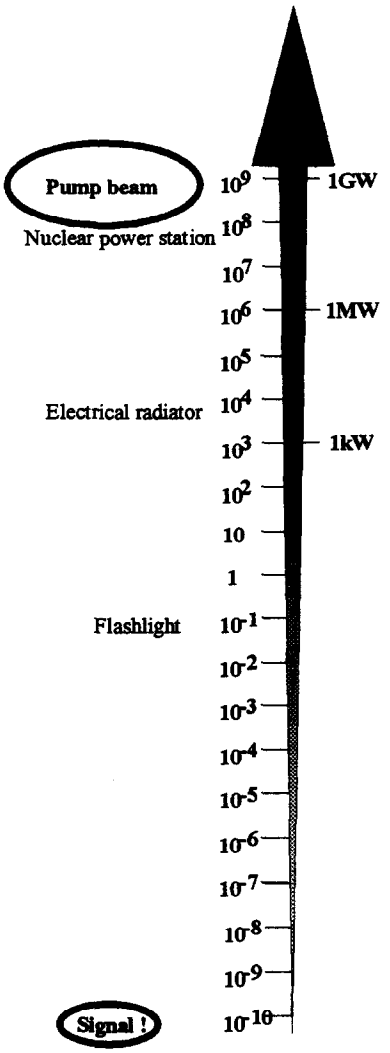

Fig. 12. Power scale.

magnetic field induced by the transient high tension of the picosecond laser device and its flash lamps.

Theoretical difficulties are also present. The most important is knowing whether the diffracted beam intensity is only a function of ΔT or not. Many obstacles are to be considered:

- non-linearity of the medium optical response, following the strong electric field;
- the stress and strain index dependence, provoked the laser pulse absorption.

Other questions that may need to be answered:

(1) What is the influence of radiative heat transfer in the medium?
(2) Which structural and/or thermal property alterations bring the electromagnetic field pulse about? (mechanical damage, chemical bond modification...).

5.2. *Device validation: slow diffusive feature of heat propagation checking* (10^{-8}–10^{-6} *s*)

A scrupulous check has been undertaken to ensure the whole device is in good working order. This validation stage is essential before examining any other heat equation than the classical one.

The heating pulse is modeled as a dirac function and heat propagation is studied on a long time scale (i.e. much longer than the medium relaxation time). The framework is consequently 'Fourier' conduction, a classical diffusive heat propagation. To prove that the device is working correctly, and that the model is appropriate, the temperature field amplitude $\Delta T(t)$, which is experimentally measured, must be exponentially decreasing, following equation (5). This has been verified.

5.3. *Typical record of* ΔT *vs time*

Figure 13 gives an example of a 'slow' experimental curve corresponding to the following values:

Beam diameter	1 mm
Interfringe	4.1 μm
Medium	Ordinary glass, 4% absorption
Sample thickness	1 mm
ΔT_0	1.8 K

An arbitrary unit diagram $\Delta T(t)$ is obtained with equation (1). The initial value $\Delta T(0)$ is estimated by an identification computing program and the dimensionless $\Delta T^*(t)$ diagram is obtained by dividing $\Delta T(t)$ by $\Delta T(0)$.

The measured diffraction efficiency is approximately 10^{-7}, that is a $4 \cdot 10^{-10}$ W signal is recorded during a few hundreds of nanoseconds. A comparatively noiseless response is obtained, although very high frequencies are recorded without any filtering.

The time scale in Fig. 13 is clearly the one of classical Fourier conduction. The difference between the diffusive model and experimental results is very small, as shown in Fig. 14. The residual is of gaussian shape, with a good zero mean value and narrow standard deviation (Fig. 15).

5.4. *Estimation of confidence intervals*

The thermal diffusivity of a sample, with previously determined thermal properties, has been estimated, using two different interfringe values (see Table 2).

In order to evaluate the influence of noise on the estimated value, a linear regression using a transformation of equation (5), $\log(\Delta T(t))$ vs time, is possible:

$$\log(\Delta T^*(t^*)) = 4\pi^2 t^*.$$

The correlation coefficient is, respectively, 0.985 and 0.970 for the experiments, according to the good residual distribution. The variance of the $\log(\Delta T(t)) = f(t)$ curve slope is a more relevant value. It permits evaluation of the confidence interval of α, with a classical confidence level of 95% (see Table 2).

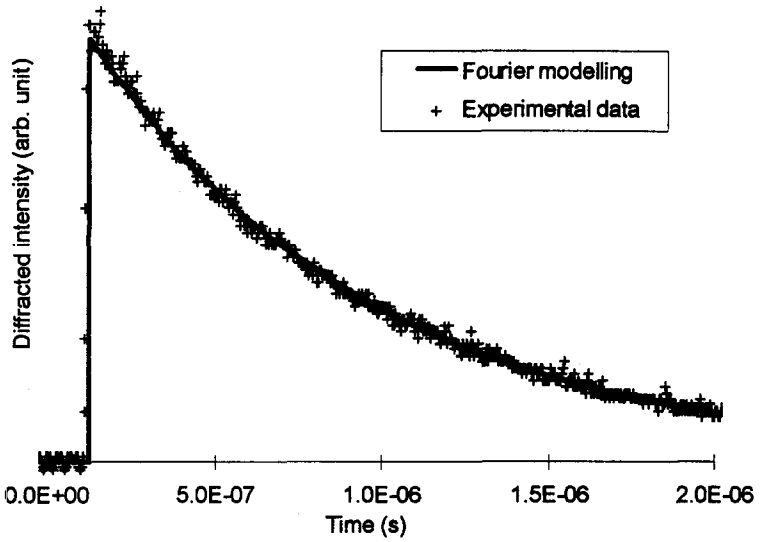

Fig. 13. Typical curve obtained from 'slow' experiment (the 17 ns heating stage is indiscernible).

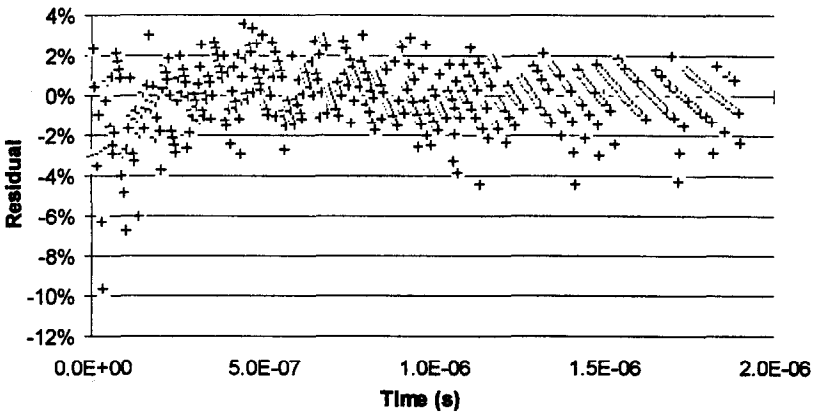

Fig. 14. Difference between modelling (Fourier conduction) and experimentation from Fig. 13.

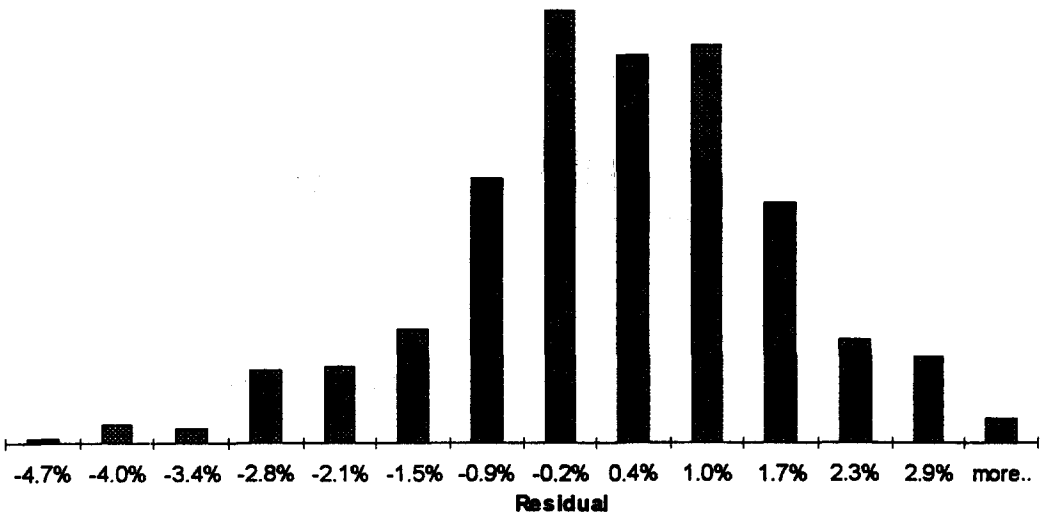

Fig. 15. Histogram of residuals from Fig. 14.

Table 2. Measured diffusivities and uncertainties

Interfringe	Estimated diffusivity	Starting line uncertainty influence ($\Delta\alpha_s$)	Noise influence ($\Delta\alpha_n$)	Angle measurement uncertainty influence ($\Delta\alpha_a$)
2.57 μm	4.68×10^{-7} m^2 s^{-1}	3%	2.2%	0.6%
3.86 μm	4.53×10^{-7} m^2 s^{-1}	3%	1.1%	1.0%

Table 3. Independent measurements of thermal properties

Thermal conductivity	0.93 W m^{-1} K^{-1}	$\pm5\%$	Guarded heat plate
Density	2442 kg m^{-3}	$\pm1\%$	Classical
Specific heat	0.785 J g^{-1} K^{-1}	$\pm3\%$	Differential scanning calorimeter

This value is relatively small, because of the great number of experimental data. Other uncertainties taking place in Table 2 included $\Delta\alpha_a$ an uncertainty on the angle between pump beams, which is about 0°05′. The uncertainty $\Delta\alpha_s$ is due to the difficult determination of the starting line (noise perturbation of signal before pump pulse).

The material properties of the sample were determined prior to our experiments by the methods outlined in Table 3. Thermal diffusivity can consequently be calculated from the above results:

$$\alpha = 4.82\times10^{-7}\ \text{m}^2\ \text{s}^{-1}\pm9\%$$

Figure 16 shows the good agreement between the experiments performed here and the previously determined properties.

5.5. *Experimental investigation of heating stage* (10^{-9}–10^{-7} *s*)

In order to investigate shorter time scale than detailed above, the first 100 ns of the event described in section 5.3 have been recorded with a 200 ps resolution (Fig. 17). The heating stage can be seen before the beginning of the diffusive process. On that time scale, the 17 ns heating pulse cannot be considered as a dirac function and analytical solution of equation (5) is no longer valid. The following system must be solved:

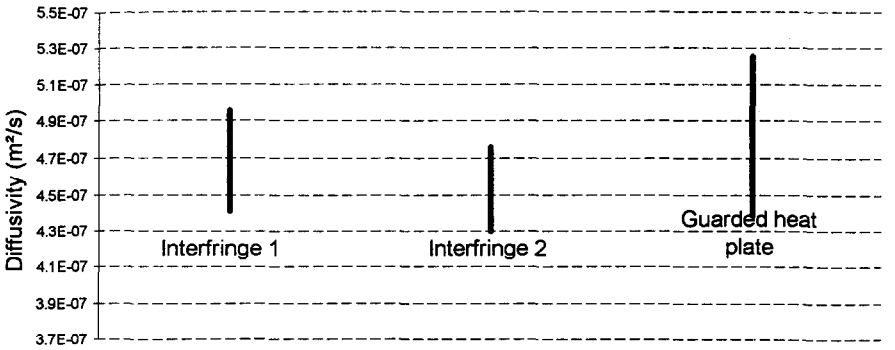

Fig. 16. Comparison of estimated and measured thermal diffusivity: F.R.S. and guarded heat plate.

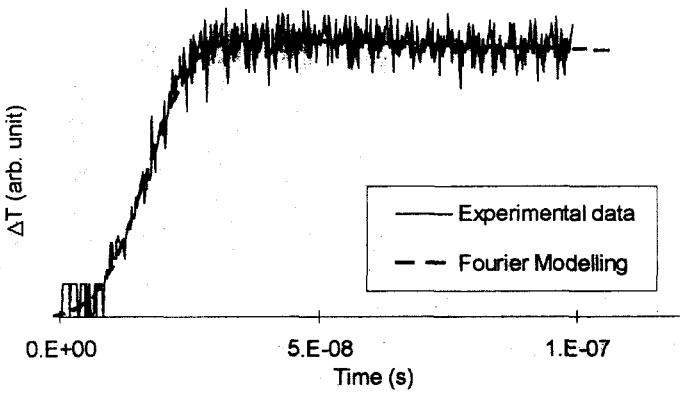

Fig. 17. Heating stage at the beginning of Fig. 13.

$$\tau\frac{\partial^2 T(y,t)}{\partial t^2}+\frac{\partial T(y,t)}{\partial t}-\alpha\frac{\partial^2 T(y,t)}{\partial y^2}=\frac{P(t)}{\rho Cp}. \quad (8)$$

Where $P(t)$ is the heat generation, due to laser pulse intensity absorption. The temporal shape is gaussian:

$$P(t)=P_0\exp\left(-\frac{t-t_c}{\frac{t_p}{2}}\right)^2$$

where t_c is the date of the middle of the pulse, t_p the pulse duration.

The initial conditions are:

$$T(y,0)=0$$

$$\frac{\partial T(y,0)}{\partial t}=0.$$

The boundary conditions are:

$$\frac{\partial T(0,t)}{\partial y}=0$$

$$\frac{\partial T(l,t)}{\partial y}=0.$$

A semi-implicit finite difference scheme (Cranck Nicholson) is used for the modelling of this stage. The value of t_p is 15 ns for the slow version of the experimentation. Knowledge of P_o and t_c is not needed because those two parameters are estimated by the identification program, following the Gauss method.

As can be seen in Fig. 17, agreement between the experimental data and the modelling is very good, even on a time scale of 10^{-9}–10^{-7} s. The Fourier law is still very well confirmed.

6. CONCLUSION

The testing and feasibility stage of this experiment have brought to light a great number of technical difficulties. Most especially, the need to come close to the limit of device specifications. Many experimental and theoretical precautions must be taken.

The first results, for a time scale on the order of 10^{-9}–10^{-6} s, are encouraging. No major obstacles have appeared concerning this ultra-short time investigation method. For the moment, the classical diffusive behavior of heat is very well confirmed, validating the experimental apparatus and the procedure.

The 'slow' experiment version, which is currently working, will soon be used to test a gas in the configuration of Fig. 11, with the aim of observing possible deviations to classical parabolic heat conduction.

Thin absorbing films and thick transparent bulks of high thermal diffusivity media are planned to be studied with the 'fast' experiment version, from 100 to 300 K, with the same goal.

REFERENCES

1. Özisik, M. N. and Tzou, D. Y., On the wave theory in heat conduction. *Journal of Heat Transfer*, 1994, **116**, 526–535.
2. Eichler, H., Enterlein, G., Munschau, J. and Stahl, H., Lichtinduzierte, thermische Phasengitter in absorbierenden Flüssigkeiten. *Zeischrift für angewandte Physik*, 1970, **31**(1), 1–4.
3. Dalil-Essakali, L., Diffusion Rayleigh et mélange à 4 ondes dans le Séléniure de Gallium. Ph.D. thesis, Université de Paris VI, Jussieu, Paris, 1994.
4. Qiu, T. Q., Juhasz, T., Suarez, C., Bron, W. E. and Tien, C. L., Femtosecond laser heating of multi-layer metals: experiments. *International Journal of Heat and Mass Transfer*, 1994, **37**(17), 2789–2797.
5. Vernotte, P., La véritable équation de la chaleur. *Comptes Rendus Hebdomadaires de Séance de l'Académie des Sciences, Paris*, 1958, **247**, 2103–2105.
6. Cattaneo, C., Sur une forme de l'equation de la chaleur éliminant le paradoxe d'une propagation instantannée. *Comptes Rendus Hebdomadaires de Séance de l'Académie des Sciences, Paris*, 1958, 431–433.
7. Vernotte, P., Les paradoxes de la théorie continue de la chaluer. *Comptes Rendus Hebdomadaires de Séance de l'Académie des Sciences, Paris*, 1958, **246**, 3154–3155.
8. Joseph, D. D. and Preziosi, L., Heat waves. *Review of Modern Physics*, 1989, **61**(1), 41–73.
9. Taitel, Y., On the parabolic, hyperbolic and discrete formulation of the heat conduction equation. *International Journal of Heat and Mass Transfer*, 1972, **15**, 369–371.
10. Jou, D., Casas-Vasquez, J. and Lebon, G., Extended irreversible thermodynamics. *Report of the Progress in Physics*, 1988, **51**, 1105–1179.